J. of Basic Sciences, Cheju Nat'l Univ.
19(2), 57~64, 2006

기초과학연구 제주대학교
19(2), 57~64, 2006

Electric-Field Induced Magnetophonon Resonance in $Hg_{1-x}Cd_xTe$

Sang Chil Lee*
Research Institute for Basic Science, Cheju National University, Jeju 690-756, Korea

The intraband magnetophonon resonances(MPR) under electric-field, and field-dependent magnetoconductivity in $Hg_{1-x}Cd_xTe$ are investigated by using the formalism of a quantum-statistical transport theory. The resonances are originated from the energy difference between Landau levels in conduction band of intraband scattering with electric field by phonons. The MPR conditions under the electric field is obtained. The qualitative features of the MPR effects under electric field are investigated as a function of the strength of magnetic field, optical phonon frequency, and the temperature. In particular, the splitting in the line shape at the MPR condition, the shift of the MPR peaks, the changes in the MPR amplitude under the electric field, and the damping or the disappearance of the peak amplitudes under the strong strength of electric field are discussed in detail.

PACS numbers: 72.20.-i, 72.20.Dp, 73.21.-b, 73.40.-c
Keywords: Magnetophonon resonance; Magnetoconductivity; Small-gap alloy semiconductor; $Hg_{1-x}Cd_xTe$

I. INTRODUCTION

The small-gap alloy semiconductor $Hg_{1-x}Cd_xTe$ has been extensively investigated during the past many years[1, 2]. The band structure of $Hg_{1-x}Cd_xTe$ by measurements of the far-infrared cyclotron resonance and of the absorption edge, and by hall and conductivity measurements has been known. The interest in these materials to date is derived primarily from the possibility of adjusting their band gap by varying the alloy composition, which makes them useful as both emitters and detectors of photons with a selectable characteristic wavelength as a detector for the infrared region at wavelengths of $\sim 10\ \mu$m[3]. $Hg_{1-x}Cd_xTe$ used as a model system to explore the basic physics of bulk and lower-dimensional narrow- and zero-gap semiconductors explorations usually focus on the very high electron mobilities in the zero-gap ($x \approx 0.1$) composition region[3–11]. Two kinds of longitudinal-optical phonons are found in the alloy composition system over a wide range of compositions, the one having the frequency of longitudinal-optical phonons in phonons in pure HgTe, and the other having the frequency of longitudinal-optical phonons in phonons in pure CdTe[12] from Raman sacttering data of $Hg_{1-x}Cd_xTe$.

Many aspects of the physics of $Hg_{1-x}Cd_xTe$ have been carried out on bulk single crystals, although some results have been reported on thin-film materials. Among these, typically, $Hg_{1-x}Cd_xTe$ is electrically characterized by measuring the low-field magnetotransport properties as a function of temperature and composition. Schmit[13] calculated the intrinsic carrier concentration, reduced Fermi energy, electron effective mass, and Fermi energy with and without doping for $Hg_{1-x}Cd_xTe$ with $x > 0.16$ and $50\ \mathrm{K} < T < 350\ \mathrm{K}$. Kahlert et.al. reported measurement of the magnetophonon reasonance (MPR) effect as a function of temperature in a confined temperature region[12]. The MPR effect is a powerful spectroscopic tool to investigate transport properties of semiconductors, such as carrier relaxation mechanism, damping of the magnetoconductivity oscillation due to the electron-phonon interaction[14], intracollisional field effects (ICFE)[15], or to determine the associated phonon energies from the periodicity with respect to the reciprocal magnetic fields of magnetoconductivity oscillation. The MPR effects under the electric field allow one to make another quantitative measurements of the scattering strength for specific Landau levels and yields direct information on the nature of the electron-phonon interaction in semiconductors. We already mentioned a theory of the MPR[14] on the basis of high-field quantum-statistical transport formula[15–19].

The purpose of the present work is to apply the field-dependent magnetoconductivity due to the phonon-assisted intraband scatterings for zero band-gap materials such as $Hg_{1-x}Cd_xTe$, which is originated from the energy difference between Landau levels in the conduction band using the formalism of a quantum-statistical transport theory, and the MPR conditions under the electric field and the magnetic field are obtained. The qualitative features of the MPR effects under the dc electric field are investigated as a function of the strength of magnetic field, optical phonon frequency, and the temperature. In particular, the splitting in the line shape at the MPR condition, the shift of the MPR peaks, the changes in the MPR amplitude under the dc electric field, and the damping or the disappearance of the peak amplitudes under the strong electric field are discussed in detail[20–25]. In this paper, we present a longitudinal-optical phonon energy versus applied magnetic field in order to get the reasonant magnetic field for the electric field as a function of temperature using the two kinds of longitudinal-optical phonon frequency of $Hg_{1-x}Cd_xTe$ revealed by experimental results. And these reasonant magnetic fields are obtained for the cases of MPR effects between intrabands as a function of the electric field.

*Electronic address: chills@cheju.ac.kr

The reat of the paper is organized as follows. In Sec. II, it is described a simple model of the system. In Sec. III, we present the field-dependent magnetoconductivity formula related to the relaxation rate, by using formalism of a quantum-statistical transport theory. In Sec. IV, the effects of MPR under the electric field is discussed. Results and conclusions are given in Sec. V.

II. MODEL OF THE SYSTEM

It is considered the transport of electron gas in the zero-gap semiconductor structure, where a static magnetic field $\vec{B} = (0, 0, B)$ and a uniform external electric field $\vec{E} = E\hat{y}$ are applied to the system. Then, the single-electron Hamiltonian for such electrons subject to the crossed electric ($\vec{E}$) and magnetic ($\vec{B}$) fields is given as follows:

$$h_{eE} = \frac{1}{2m^*}\left(\vec{p} + e\vec{A}\right)^2 + eEy, \tag{2.1}$$

where $\vec{A}$ is the vector potential, $\vec{p}$ is the momentum operator, m^* represents the effective mass of an single-electron. By taking into account the Landau gauge of vector potential $\vec{A} = (-yB, 0, 0)$, the one-electron normalized eigenfuncitons ($< \vec{r} \mid \lambda >$) and eigenvalues (E_λ) are given, respectively, by

$$< \vec{r} \mid \lambda > \equiv < \vec{r} \mid N, k_x, k_z > = U_0(\mathbf{r})F_\lambda(\mathbf{r}), \tag{2.2}$$

$$E_\lambda = E_N(k_x, k_z) = \varepsilon_\lambda(\vec{k}) + eEy_\lambda + \frac{1}{2}m^*V_d^2, \tag{2.3}$$

with

$$\varepsilon_\lambda(\vec{k}) = (N + \frac{1}{2})\hbar\omega_s + \frac{\hbar^2 k_z^2}{2m^*}, \tag{2.4}$$

and

$$y_\lambda = l_B^2[k_x - m^*V_d/\hbar], \tag{2.5}$$

where λ denotes the Landau state $(N, \vec{k})$, $N(= 0, 1, 2, \cdots)$ are the Landau-level indices, $\vec{r}$ is the position vector of an single-electron with momentum $\vec{p}$ and effective mass m^*, k_x and k_z are, respectively, the wavevector components of the electron in the x and z direction, $\omega_s(= eB/m^*)$ is the cyclotron frequency, $l_B = (\hbar/m^*\omega_s)^{1/2}$ is the radius of the ground Landau orbit, and $V_d(= E/B)$ is the drift velocity. Also in Eq. (2.2), $U_0(\vec{r})$ denotes the Bloch function at $\vec{k} = 0$ and $F_\lambda(\vec{r})$ is the envelope function given by[16]

$$F_\lambda(\vec{r}) = \frac{1}{\sqrt{L_x L_z}}\phi_N(y - y_\lambda)\exp(ik_x x + ik_z z). \tag{2.6}$$

Here $\phi_N(y)$ in Eq. (2.6) is the eigenfunctions of the simple harmonic oscillator, and L_x and L_z are, respectively, the x and z directional normalization lengths. It is assumed that the Bloch function $U_0(\vec{r})$ and the envelope function $F_\lambda(\vec{r})$ are, respectively, normalized in the crystal as

$$\int_C U_0^*(\vec{r})U_0(\vec{r})d^3r = 1, \tag{2.7}$$

$$\int_\Omega F_{\lambda'}^*(\mathbf{r})F_\lambda(\mathbf{r})d^3r = \delta_{\lambda'\lambda} = \delta_{N'N}\delta_{k_x'k_x}\delta_{k_z'k_z}, \tag{2.8}$$

where C is the volume of the unit cell and $\Omega(= L_xL_yL_z)$ is the crystal volume in the real space.

Applying the above results, the energy eigenvalues for the conduction band from Eqs.(2.3) and (2.4) is given by

$$E_\lambda = E_g + (N + 1/2)\hbar\omega_s + \frac{\hbar^2 k_z^2}{2m^*} + eEy_\lambda + \frac{m^*}{2}V_d^2, \tag{2.9}$$

where E_g is the energy gap. We see from Eq. (2.9) that in the presence of the magnetic field and the zero electric field, the conduction and valence bands separated at $\vec{k} = 0$ by the direct-band-gap E_g are splitted into Landau subbands.

III. FIELD-DEPENDENT MAGNETOCONDUCTIVITY ASSOCIATED WITH RELAXATION RATES

We want to evaluate the field-dependent magnetoconductivity $\sigma_{yy}(E)$ for the system modeled in the previous section by applying the eigenfunctions and eigenvalues given in Eqs. (2.2) and (2.3) and using the general expression of the nonlinear dc conductivity $\sigma_{kl}(E)(k, l = x, y, z)$ derived in Ref. 15. Then, the magnetoconductivity $\sigma_{yy}(E)$ can be easily obtained from Eq. (4.38) of Ref. 15 as follows:

$$\sigma_{yy}(E) = \frac{\hbar}{\Omega}\sum_\lambda\sum_{\lambda'} |< \lambda \mid j_y \mid \lambda' >|^2 \frac{f(\epsilon_\lambda) - f(\epsilon_{\lambda'})}{\varepsilon_\lambda - \varepsilon_{\lambda'}} A_{\lambda'\lambda}(E) \tag{3.1}$$

with

$$A_{\lambda'\lambda}(E) = \frac{\Gamma_{\lambda'\lambda}(E)}{(E_\lambda - E_{\lambda'} - \nabla_{\lambda\lambda'}(E))^2 + \Gamma_{\lambda'\lambda}^2(E)}, \tag{3.2}$$

where j_y is the y component of a single-electron current operator, $f(\epsilon_\lambda)$ denotes the Fermi-Dirac distribution function for hot-electrons associated with the eigenstate of Eq. (2.2) and the eigenvalue of Eq. (2.4), $\nabla_{\lambda\lambda'}(E)$ is the shift of spectral line shape by the oscillatory behavior of the hot electron MPR, and the field-dependent relaxation rate $\Gamma_{\lambda'\lambda}(E)$, which appears in terms of the

collision broadening due to the electron-phonon interaction, play a role of the width in the spectral line shape. Note that ε_λ and E_λ are nearly the same for relatively high electric-field case in which ICFE effects are not effective. However, for sufficiently high electric-field case in which ICFE effects are effective, ε_λ and E_λ are, respectively, given by Eqs. (2.3) and (2.4), where we considered the electric field applied to the y direction alone. In the direct intraband transitions, the matrix elements of the single-electron current operator in Eq. (3.1) are given, in terms of Eq. (2.2), by

$$|\langle\lambda \mid j_y \mid \lambda'\rangle|^2 = \frac{e^3\hbar B}{2m^{*2}}\left((N+1)\,\delta_{N'N+1} + N\delta_{N'N-1}\right) \times \delta_{k_z k_z'}\delta_{k_s k_s'}, \tag{3.3}$$

where the Kronecker symbols $(\delta_{N'N}\delta_{k_z k_z'}\delta_{k_s k_s'})$ denote the selection rules.

In order to get the magnetoconductivity, it is necessary to calculate the matrix elements of the relaxation rate Γ. Within the first-order Born approximation of scattering processes, the matrix elements of Γ associated with the direct transition between the states $\mid\lambda>$ and $\mid\lambda'>$ is generally given by

$$\Gamma_{\lambda\lambda'}(E) = \pi\sum_{\vec{q}}[(N_{\vec{q}}+1)S_+(E) + N_{\vec{q}}S_-(E)], \tag{3.4}$$

where $N_{\mathbf{q}}$ is the Bose-Einstein distrbution function for phonon with energy $\hbar\omega_{\vec{q}}$, and $S_\pm(E)$ is given by

$$S_\pm(E) = \sum_{\lambda_3}{}'[|\langle\lambda \mid \gamma_{\vec{q}}^{\mp} \mid \lambda_3\rangle|^2\,\delta(E_{\lambda_3} - E_{\lambda'} \pm \hbar\omega_{\vec{q}}) + |\langle\lambda_3 \mid \gamma_{\vec{q}}^{\pm} \mid \lambda'\rangle|^2\,\delta(E_{\lambda_3} - E_\lambda \pm \hbar\omega_{\vec{q}})] \tag{3.5}$$

Here $\gamma_{\vec{q}}(= C(\vec{q})\exp(i\vec{q}\cdot\vec{r}))$ represents the one-electron operator. The phonons couple to the electron via the interaction potential $C(\vec{q})$, the form of which depends on the type of interaction. It should be noted that the prime on the summation sign in Eq. (3.5) indicates the exclusion of the diagonal element of $\gamma_{\vec{q}}$, and $\sum_{\lambda_3}$ represents the triple summations $\sum_N\sum_{k_y}\sum_{k_z}$ for intraband scattering of the conduction band. Also in Eq. (3.5), the δ-functions express the law of energy conservation in one-phonon collision (emission and absorption) processes, where the effect of the electric field is included exactly through the eigenvalue E_λ of an electron. The energy-conserving δ functions in Eq. (3.5) imply that when the electron undergoes a collision by absorbing the energy from the field, its energy can only change by an amount equal to the energy of a phonon involved in the transition. This in fact leads to electric-field-induced MPR. If we take the limit $E \to 0$ in Eq. (3.5), the expression reduces to the usual instantaneous phonon emission and absorption processes for zero-gap materials. In the representation of Eq. (2.2), the matrix elements in Eq. (3.5) are given by

$$|\langle\lambda \mid \gamma_{\vec{q}}^{\mp} \mid \lambda'\rangle|^2 = |\,C(\vec{q})\,|^2\,|\,J_{NN'}(u)\,|^2\,\delta_{k_z k_z' \pm q_z}\delta_{k_z k_z' \pm q_z}, \tag{3.6}$$

where $|\,J_{NN'}(u)\,|^2$ is given by

$$|\,J_{NN'}(u)\,|^2 = \frac{N_n!}{N_m!}\exp(-u)u^{N_m-N_n}[L_{N_n}^{N_m-N_n}(u)]^2 \tag{3.7}$$

with

$$u = (l_B^2/2)[q_x^2 + q_z^2]. \tag{3.8}$$

Where $N_n = \min(N, N')$, $N_m = \max(N, N')$, and $L_m^n(u)$ is the associated Laguerre polynomial.

For intraband scattering associated with the electronic transition between the states $|N+1, k_x, k_z>$ and $|N, k_x, k_z>$, we obtain as follows:

$$S_\pm = |C(\vec{q})|^2 \sum_{N', k_x', k_z' \neq N, k_x, k_z} |J_{N+1N'}(u)|^2\,\delta\left[(N-N')\,\hbar\omega_s + \frac{\hbar^2 k_z^2}{2m_z^*} - \frac{\hbar^2\,(k_z \mp q_z)^2}{2m_z^*} \mp \hbar V_d q_z \mp \hbar\omega_{\mathbf{q}}\right] + |C(\vec{q})|^2 \sum_{N', k_x', k_z' \neq N, k_x, k_z} |J_{NN'}(u)|^2\,\delta\left[(N'-N-1)\,\hbar\omega_s - \frac{\hbar^2 k_z^2}{2m_z^*} + \frac{\hbar^2\,(k_z \pm q_z)^2}{2m_z^*} \mp \hbar V_d q_z \pm \hbar\omega_{\mathbf{q}}\right], \tag{3.9}$$

where N' indicates the intermediate localized Landau level indices, and $C(\vec{q})$ is the Fourier transform of the electron-phonon interaction potential.

To calculate the $S_\pm$ of Eq. (3.9) for electron-phonon interaction, we consider the Fourier component of the interaction potentials for polar longitudinal optical phonon scattering given by $|C(q)|^2 = D'/(\Omega q^2)$ with D' being the constant of the polar interaction, where the assumption that the phonons are dispersionless (i.e., $\hbar\omega_{\vec{q}} \approx \hbar\omega_{LO} \approx$ constant, where ω_{LO} is the longitudinal optical phonon frequency) was made. As shown in Eq. (3.9), the $S_\pm$ involves the summation with respect to k_z and k_z and integrations with respect to q_x, q_y, and q_z in Cartesian coordinates. The summation with re-

spect to k_x and k_z is replaced by the following relation: $\sum_{k_x k_z} = \frac{L_x L_z}{4\pi^2}\int_{-m^*\omega_s L_y/2\hbar+eF/\hbar\omega_s}^{m^*\omega_s L_y/2\hbar+eF/\hbar\omega_s} dk_x \int_{-\pi/a}^{\pi/a} dk_z()$. In addition, we assume that the Fermi-Dirac distribution function can be replaced by the Boltzmann distribution function for nondegenerate semiconductor, i.e., $f[E_N(k_x,k_z)] \approx \exp\{\beta[\mu - E_N(k_x,k_z)]\}$, where μ denotes the chemical potential given by

$$\mu = (1/\beta)\ln[\sqrt{2\pi^3 n_e^2 L_y^2 \beta^3 \hbar^4 V_d^2/m^*}\,\sinh(\beta\hbar\omega_s/2)\,/\,\sinh[(\beta m^*\omega_s V_d L_y/2)]].$$

Here $n_e = N_e/V$ denotes the electron density. The integral over q_x, q_y, and q_z is very difficult to evaluate analytically since it must be done separately for each N and N'.. So, to simplify the calculations, we replace $\hbar V_d q_x$ in the argument of the δ function by the potential energy difference $eE\Delta\bar{y}$ across the spatial extent $\Delta\bar{y}$ of a Landau state as some authors do[26, 27]. Then, the relaxation rates associated with the electronic transition between the states $|N+1, k_x, k_z\rangle$ and $|N, k_x, k_z\rangle$ can be expressed as

$$\begin{aligned}\bar{\Gamma} = \frac{D'}{4\pi}\sqrt{\frac{m^*}{2\hbar^2}}\sum_{N'\neq N}\sum_{\pm}\{(N_{\bar{q}}+1)\left(\frac{K_1^{\pm}(N,N';k_z)\,\theta(\Theta_1(k_z))}{\sqrt{\Theta_1(k_z)}}+\frac{K_3^{\pm}(N,N';k_z)\,\theta(\Theta_3(k_z))}{\sqrt{\Theta_3(k_z)}}\right)\\ +N_{\bar{q}}\left(\frac{K_2^{\pm}(N,N';k_z)\,\theta(\Theta_2(k_z))}{\sqrt{\Theta_2(k_z)}}+\frac{K_4^{\pm}(N,N';K_z)\,\theta(\Theta_4(k_z))}{\sqrt{\Theta_4(k_z)}}\right)\},\end{aligned} \tag{3.10}$$

where $\theta(x)$ is the Heaviside step function defined by $\theta(x) = 1$ for $x \geq 0$ and 0 for $x < 0$, and

$$\Theta_1(k_z) = (N-N')\hbar\omega_s + \frac{\hbar^2 k_z^2}{2m^*} - eF\sqrt{\hbar/m^*\omega_{LO}} - \hbar\omega_{LO}, \tag{3.11a}$$

$$\Theta_2(k_z) = (N-N')\hbar\omega_s + \frac{\hbar^2 k_z^2}{2m^*} + eF\sqrt{\hbar/m^*\omega_{LO}} + \hbar\omega_{LO}, \tag{3.11b}$$

$$\Theta_3(k_z) = +(N'-N-1)\hbar\omega_s - \frac{\hbar^2 k_z^2}{2m^*} - eF\sqrt{\hbar/m^*\omega_{LO}} + \hbar\omega_{LO}, \tag{3.11c}$$

$$\Theta_4(k_z) = +(N'-N-1)\hbar\omega_s - \frac{\hbar^2 k_z^2}{2m^*} + eF\sqrt{\hbar/m^*\omega_{LO}} - \hbar\omega_{LO}, \tag{3.11d}$$

and

$$K_1^{\pm}(N,N';K_z) = \frac{1}{2}\int_0^{\infty} du_{\perp}\,|J_{N+1N'}(u)|^2\,\frac{1}{u+a_{1\pm}^2}, \tag{3.12a}$$

$$K_2^{\pm}(N,N';K_z) = \frac{1}{2}\int_0^{\infty} du_{\perp}\,|J_{N+1N'}(u)|^2\,\frac{1}{u+a_{2\pm}^2}, \tag{3.12b}$$

$$K_3^{\pm}(N,N';K_z) = \frac{1}{2}\int_0^{\infty} du_{\perp}\,|J_{NN'}(u)|^2\,\frac{1}{u+a_{3\pm}^2}, \tag{3.12c}$$

$$K_4^{\pm}(N,N';K_z) = \frac{1}{2}\int_0^{\infty} du_{\perp}\,|J_{NN'}(u)|^2\,\frac{1}{u+a_{4\pm}^2} \tag{3.12d}$$

with $a_{i\pm}^2 = l_B^2\left(k_z \pm \sqrt{2m^*\Theta_i(k_z)/\hbar^2}\right)^2/2$. In order to obtain Eq. (3.11), we transformed the sum over $\vec{q}$ in Eq. (3.4) into an integral form in the usual

way as $\sum_q \rightarrow (V/(2\pi)^3)\int_{-\infty}^{\infty}\int_{-\infty}^{\infty}\int_{1st\ BZ} dq_x dq_y dq_z$ and used the following property of the Dirac delta function: $\delta[f(x)] = \sum_i \delta[x - x_i]/|f'(x_i)|$ with x_i being the roots of $f(x)$, and the approximaton[26, 27] $eF\Delta y \approx eF\sqrt{\hbar/m^*\omega_{LO}}$. It is clearly seen from Eq. (3.11) that the relaxation rates diverge whenever the conditions $\Theta_i(K_z) = 0$ and $a_{i\pm}^2 = 0$ in $K_i^{\pm}(N, N'; t)$ are satisfied. From these conditions, the relaxation rates [and hence, the frequency-dependent magnetoconductivities $\sigma_{yy}(F)$] for polar LO-phonon scattering show the resonant behaviors at $P\hbar\omega_s = \hbar\omega_{LO} \pm eF\sqrt{\hbar/m^*\omega_{LO}}$ ($P \equiv N' - N = 1, 2, 3, ...$). When the MPR conditions are satisfied in the course of scattering events, the electrons in the Landau levels specified by the level index (N) can make transitions to one of the Landau levels (N') by absorbing and/or emitting a photon of energy $\hbar\omega$ during the absorption of a LO phonon of energy $\hbar\omega_{LO}$.

The peak positions strongly depend on the difference of Landau-level indices in the intraband scattering, and the difference in the effective mass between the conduction bands and valence bands and on the strength of the electric field in the intraband scattering by phonons. If we take the limit $F \rightarrow 0$ in Eq. (3.9) the expression becomes resonance conditions for the ordinary intraband MPR, which is the same result used by Nicolas[4] for theoretical values, where only phonon emission processes is assumed.

It is noted that the matrix elements due to the intraband scatterings for zero band-gap materials are included in Eq. (3.11) since phonon energy $\hbar\omega_{\vec{q}}$ is much larger than the zero band-gap. For the case that phonon energy is much smaller than the band-gap E_g, the term due to the phonon-assisted interband scatterings can be neglected. We further notice that the matrix elements due to the intraband scattering through the δ function of Eq. (3.9) give us to obtain the intraband MPR. For simplicity, we now restrict ourself to the case of the matrix elements due to the intraband scatterings, and the electric-field-induced MPR to see the magnetoconductivity. It should be noted that we did not perform the calculation of the amplitude of oscillation because we were interested in the electric-field-induced MPR peak positions.

IV. NUMERICAL RESULTS

In this section, we present the numerical results of the field-dependent magnetoconductivity formula $\sigma_{yy}(E)$ in Eq. (3.1), which is related to the MPR for the bulk materials, and analyze these results with the increasing strength of the electric field and the increasing temperature. According to Raman scattering data, two kinds of longitudinal-optical phonons of $Hg_{1-x}Cd_xTe$ are found in the alloy system over a wide range of compositions, the one ($\hbar\omega_{LO} = 17.1$ meV) is the frequency of LO phonons in pure HgTe , and the other ($\hbar\omega_{LO} = 19.6$ meV) is the frequency of LO phonons in pure CdTe. In calculation we use the parameters obtained from the experimental and theoretical results[3, 12]. We use the value of energy gap $:E_g(x,T) = -0.302 + 1.93x + 5.35 \times 10^{-4}T(1-2x) - 0.81x^2 + 0.832x^3$(eV), obtained from the results fitted[13]. The composition used in calculation is $x = 0.3$, and the effective mass of conduction band as a function of temperature is $(3.199 \times 10^{-16} n_i T^{-3/2} \exp(E_g/(2k_BT)))^{\frac{1}{3}}$[13] at $T =$ 100 K. In addition, the electron density

$$n_e = 10^{14}\left(5.585 - 3.82x + 1.753 \times 10^{-3}T - 1.364 \times 10^{-3}xT\right) E_g^{3/4} T^{3/2} e^{-E_g/(2k_BT)}$$

[13], the constant of the polar interaction $D' = 5.2 \times 10^{-50}$ $kg^2m^7s^{-4}$ and twenty-one Landau levels are included in the calculation of the field-dependent magnetoconductivity.

Figure 1 shows the dependence of the electric-field strength of the MPR($E \neq 0$) peak amplitudes in the magnetoconductivities $\sigma_{yy}(E)$ for the various temperatures, respectively, at the composition $x = 0.3$ and the two different optical phonon energies as a function of the strength of magnetic field $B = 1, 2$, and 3 T, respectively. It is very interesting to note that the gradually damping phenomena of the MPR peak amplitudes is shown with increasing strength of the electric field, which is compared with the results that the peak amplitude of MPR is damped at the high electric field predicted by Baker, Mori et. al., and Wakahara et. al.[20, 22, 24]. As the strength of the magnetic field and the optical phonon energy are increased, and the temperature is decreased in Fig. 1, the critical strength of the electric-field due to the strong damping or the disappearance of the MPR peak amplitude is increased.

Figure 2 shows the resonant magnetic-field strength due to each transition for the various electric-field strength at the various temperatures $T = 200$, 250, and 300 K, where all MPR($E \neq 0$ or $E = 0$) peaks including the subsidiary peaks, respectively, in Fig.1 are assigned from the crossing point giving the resonant magnetic field in Fig. 2. It is seen from the figure that as the difference of Landau-level indices is increased, and the temperature and the optical phonon energy is decreased, all MPR peak positions including the subsidiary peak positions are shifted to the lower magnetic field side. It is also shown that the shifts of all MPR peaks($E \neq 0$ or $E = 0$) are increased as the electric-field strength is increased, and the increase of MPR($E \neq 0$) peak shift is the largest in the case of $P = 1$.

Figure 3 shows the dependence of the MPR($E \neq 0$) peak shifts on the electric field according to the differ-

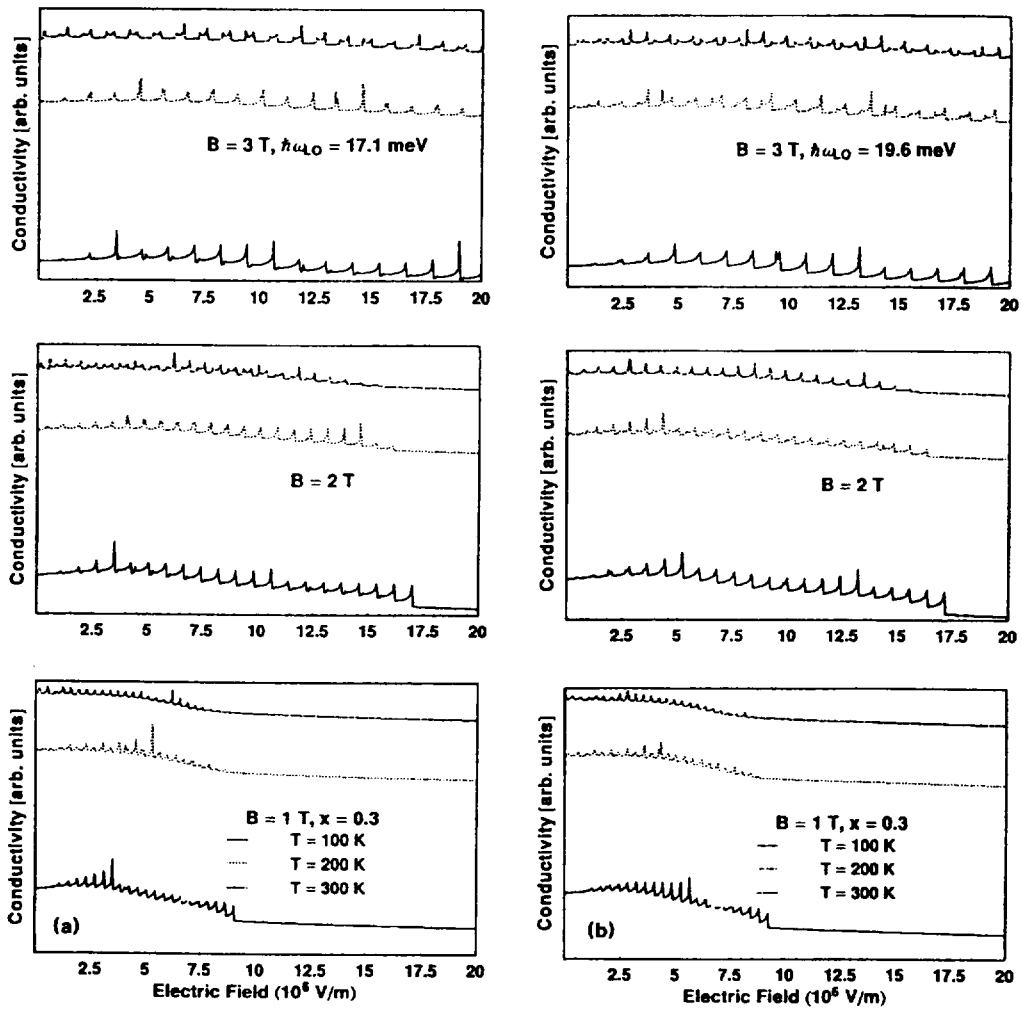

FIG. 1: Spectral line shapes of the magnetoconductivity $\sigma_{yy}(E)$ as a function of the strength of the applied electric field for the various strength of the magnetic field at the composition $x = 0.3$. The solid, dotted, and dashed lines are for $T = 100, 200$,and 300 K, respectively.

ence of Landau-level indices for the various temperatures $T = 150$, 200, 250, and 300 K. From Fig. 3, the shifts of MPR($E \neq 0$) peak positions are increased as the electric-field strength is increased and the difference in the Landau level indices is decreased, as expected in Fig. 1. In Fig. 3, the magnitude of the slope of the resonance field shifts for the strength of the electric-field is increased as the temperature is increased because of the temperature dependence of the effective mass of conduction band. These results shown in Figs. 1, 2, and 3 are in good agreement with those of others[20, 22, 24].

V. CONCLUSIONS

Up to now, we have presented the field-dependent magnetoconductivity $\sigma_{yy}(E)$ accompanied with the electric-field-induced MPR related to the phonon-assisted intraband scatterings, and analyzed these results with the strength of the electric field and the temperature using the parameters obtained from the experimental and theoretical results, and obtained the MPR condition $P\hbar\omega_c = \hbar\omega_{LO} \pm eE\sqrt{\hbar/m^*\omega_{LO}}$ $(P \equiv N' - N = 1, 2, 3, ...)$ as a

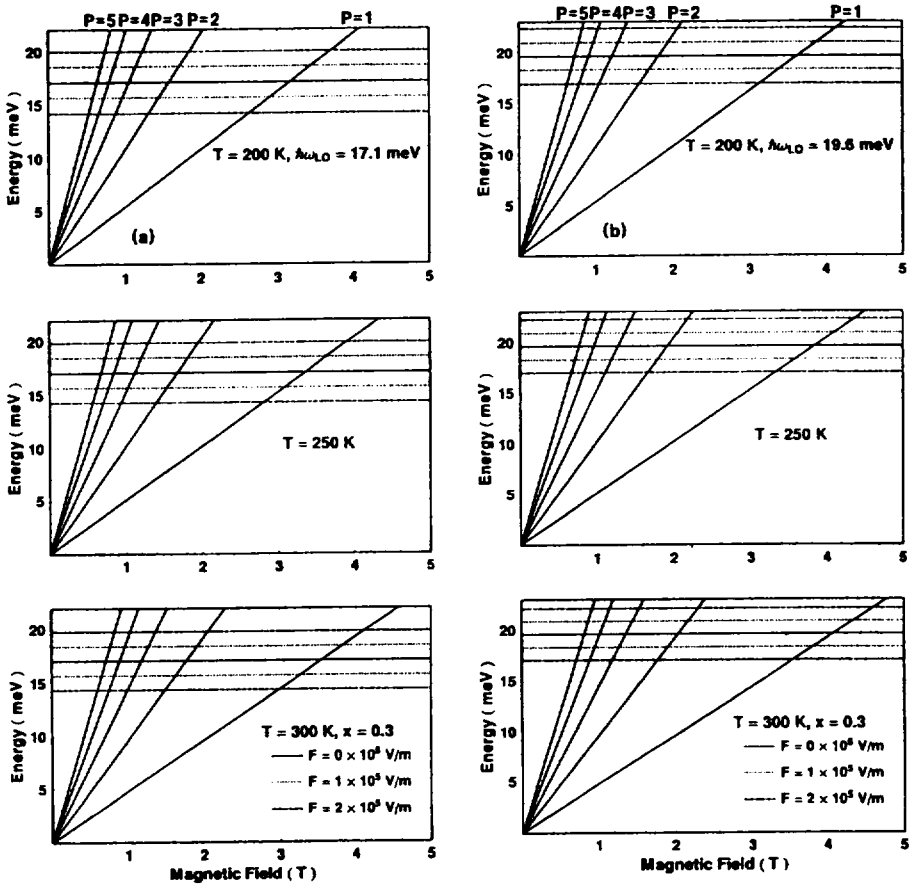

FIG. 2: Energy versus strength of the applied magnetic field for the various temperature at the composition $x = 0.3$. The solid, dotted, and dashed lines are for $E = 0 \times 10^5, 1 \times 10^5$, and 2×10^5 V/m, respectively. Here the crossing points indicate the resonant magnetic field.

function of strength of magnetic field, strength of electric field, and temperature. In particular, we have studied the variation of the anomalous behavior of the MPR line shape such as the splitting of the MPR peaks, the appearance of the subsidiary MPR peaks, the strong damping or the disappearance of the MPR peak amplitudes with increasing strength of the electric field, and the shift of MPR peaks due to the strength of the incident electric field. All peaks are observed at the value satisfied by the MPR condition ($P\hbar\omega_c = \hbar\omega_{LO}$) and the MPR condition under the electric field given by $P\hbar\omega_c = \hbar\omega_{LO} \pm eE\sqrt{\hbar/m^*\omega_{LO}}$ ($P \equiv N' - N = 1, 2, 3, ...$) at the magnetic field. As the strength of the electric field is increased, the width of splitting of the subsidiary MPR peaks obtained from the condition($P\hbar\omega_c = \hbar\omega_{LO} \pm eE\sqrt{\hbar/m^*\omega_{LO}}$) splitted from the MPR peaks($E = 0$) is increased and the shift of the MPR peak positions is increased. As the difference of Landau-level indices is increased, the MPR peak positions are shifted to the lower magnetic field side. As the temperature and the phonon energy is increased, the MPR peak positions are shifted to the higher magnetic field side. The shifts of all MPR peaks($E \neq 0$ or $E = 0$) are increased as the electric-field strength is increased. As the temperature is increased, the critical value of strength of the electric field at the strong damping or the disappearance of the MPR peak amplitude is decreased. Throughout this work, the single-particle picture has been used. Thus, electron-electron interactions have been ignored. Despite the above shortcomings of the theory, we expect that our results will help to understand the MPR effects under the dc electric field in semiconductor.

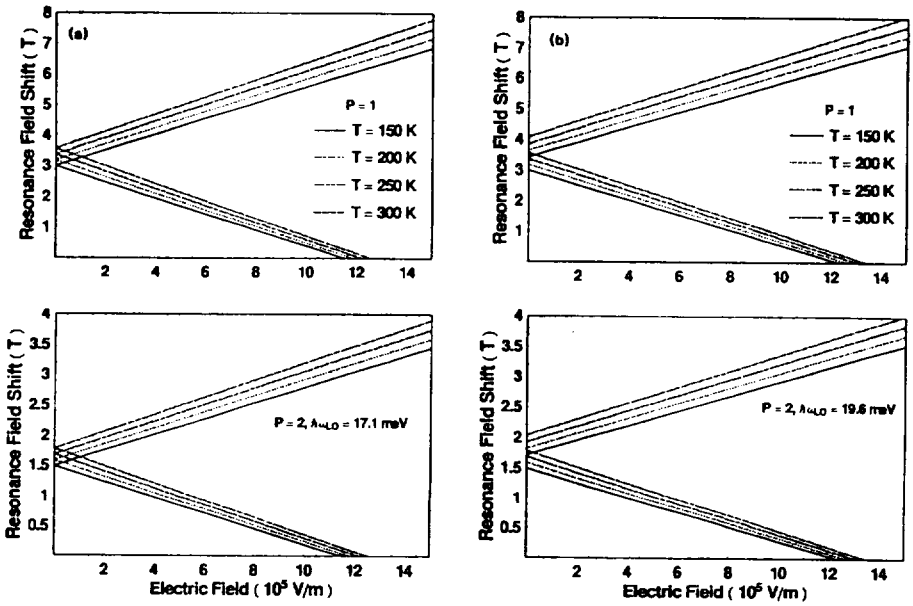

FIG. 3: Dependence of the resonance field shift on the strength of the electric-field for the $P = 1$ and 2 transition. The solid, dotted, dashed, and dashed-dotted lines are for $T = 150, 200, 250$,and 300 K, respectively.

[1] R. Dornhaus and G. Nimtz, Narrow-gap semiconductors, springer Tracts in Modern Physics Vol. 98(Springer-Verlag, New york, 1983), p. 119 ff.

[2] W. E. Tennant, C. A. Cockrum, J. B. Gilpin, M. Z. Kinch, M. B. Reine, and R. P. Ruth, J. Vac. Sci. Technol. B 10, 1359(1992).

[3] Tineke Thio, S. A. Solin, J. W. Bennett, and D. R. Hines, Phys. Rev. B57, 12239(1998).

[4] R. J. Nicholas, Prog. Quant. Electr., **10**, 1 (1985).

[5] D. Schneider, C. Brink, G. Irmer, and P. Verma, Physica B 256, 625(1998).

[6] P. Warmenbol, F. M. Peeters, and J. T. Devreese, Phys. Rev. B39, 7821(1989);37, 4694(1988).

[7] N. Mori, H. Momose, and C. Hamaguchi, Phys. Rev. B45, 4536(1992).

[8] J. Y. Ryu and R. F. O'Connell, Phys. Rev. B48, 9126(1993);J. Y. Ryu, G. Y. Hu, and R. F. O'Connell, ibid. 49, 10437(1994).

[9] A. Suzuki and M. Ogawa, J. Phys. C10, 4659(1998).

[10] G. Ploner, J. Smoliner, G. Strasser, M. Hauser, and E. Gornik, Phys. Rev. B57, 3966(1998).

[11] S. C. Lee, J. Y. Ryu, S. W.Kim, and C. S. Ting, Phys. Rev. B62, 5045(2000).

[12] H. Kahlert and G. Bauer, Phys. Rev. Lett., 30, 1211(1973).

[13] J. L. Schmidt, J. of Appl. Phys., 41, 2876(1970).

[14] S. C. Lee, Y. B. Kang, G. Y. Hu, J. Y. Ryu, and S. D. Choi, Phys. Rev. B57, 11875(1998).

[15] J.Y. Ryu and S.D. Choi, Phys. Rev. **B44**, 11328 (1991).

[16] S. Y. Choi, S. C. Lee, H. J. Lee, H. S. Ahn, S. W. Kim, and J. Y. Ryu, Phys. Rev. B 66, 155208 (2002);S. C. Lee, H. S. Ahn, D. S. Kang, S. O. Lee and S. W. Kim, Phys Rev. B67, 115342(2003).

[17] J. Y. Ryu, Y. C. Chung, and S. D. Choi, Phys. Rev. B32, 7769(1985).

[18] J. Y. Ryu, and S. D. Choi, Prog. Theor. Phys. 72, 429(1984).

[19] S. D. Choi and O. H. Chung, Solid State commun. 46, 717(1983).

[20] J. R. Barker, Solid State Electron. **21**, 197 (1978).

[21] L. Eaves, P. S. S. Guimaraes, J. C. Portal, T. P. Pearsall, and G. Hill, Phys. Rev. Lett. **53**, 608 (1984): L. Eaves, P. S. S. Guimaraes, J. C. Portal, J. Phys. C **17**, 6177 (1984).

[22] N. Mori, N. Nacamura, K. Taniguchi and C. Hamaguchi, J. Phys. Soc. Jpn. **57**, 205 (1988).

[23] R. Kubo, J. Phys. Soc. Jpn. **12**, 570 (1957).

[24] S. Wakahara and T. Ando, J. Phys. Soc. Jpn. **61**, 1257 (1992).

[25] A. Suzuki, Physica B **183**, 191 (1993).

[26] P. Vailopoulos, M. Charbonneau and C. M. Van Vliet, Phys. Rev. B **35**, 1334 (1987).

[27] A. Suzuki, Phys. Rev. B **45**, 6731 (1992).